Surface Nanobubbles Are Stabilized by Hydrophobic Attraction

Tan, Beng Hau; An, Hongjie; Ohl, Claus-Dieter

2018

Tan, B. H., An, H., & Ohl, C.-D. (2018). Surface Nanobubbles Are Stabilized by Hydrophobic Attraction. Physical Review Letters, 120(16), 164502-.

https://hdl.handle.net/10356/88750

https://doi.org/10.1103/PhysRevLett.120.164502

Surface Nanobubbles Are Stabilized by Hydrophobic Attraction

Beng Hau Tan (陈明豪),[1,2,*] Hongjie An (安红杰),[1,†] and Claus-Dieter Ohl[1,3,‡]
[1]*Cavitation Lab, Division of Physics and Applied Physics, School of Physical and Mathematical Sciences, Nanyang Technological University, 21 Nanyang Link, 637371 Singapore, Singapore*
[2]*School of Mechanical and Aerospace Engineering, Nanyang Technological University, 50 Nanyang Avenue, 639798 Singapore, Singapore*
[3]*Department for Soft Matter, Institute of Physics, Otto-von-Guericke University Magdeburg, 39106 Magdeburg, Germany*

(Received 21 January 2018; published 19 April 2018)

The remarkably long lifetime of surface nanobubbles has perplexed researchers for two decades. The current understanding is that both contact line pinning and supersaturation of the ambient liquid are strictly required for the stability of nanobubbles, yet experiments show nanobubbles surviving in open systems and undersaturated environments. We find that this discrepancy can be addressed if the effects of an attractive hydrophobic potential at the solid substrate on the spatial distribution of the gas concentration is taken into account. We also show that, in our model, only substrate pinning is strictly required for stabilization; while hydrophobicity and supersaturation both aid stability, neither is mandatory—the absence of one can be compensated by an excess of the other.

DOI: 10.1103/PhysRevLett.120.164502

Spherical gas bubbles grow or shrink depending on the concentration of the dissolved gas of the surrounding liquid. This process is governed by the Epstein and Plesset [1] theory, which models the transport of gas with the diffusion equation. The Epstein-Plesset theory is widely accepted because it exhibits excellent agreement with experiments on bubbles with radii as small as $R \sim 5$–$10\ \mu$m [2,3]. Under standard conditions, the bubbles shrink over the diffusion timescale $\tau \sim R^2/D$ (where D is the diffusion constant), which is several seconds for a microbubble and subsecond for a nanobubble. Remarkably, however, over the past two decades, various groups have reported surface-attached nanobubbles (radius of curvature $R \sim 1\ \mu$m) [4–6] on immersed substrates, which survive for at least several *days*.

Numerous hypotheses have been proposed to account for the stability of surface nanobubbles. It has variously been suggested that the bubbles are protected by a gas-impermeable layer of contamination [7] or that the strong Epstein-Plesset outflux from the nanobubble is compensated by an influx at the contact line [8,9], but most of these models were eventually ruled out by experiments [10–12].

In the current understanding, the experimentally observed contact line pinning [13,14] and supersaturation of gas in the liquid are both considered necessary for the stabilization of nanobubbles. This idea was first introduced to the literature by the thermodynamic calculations of Liu and Zhang [15,16]. Later, by modifying the Epstein-Plesset theory for pinned surface nanobubbles, Lohse and Zhang [17] and Chan, Arora, and Ohl [18] independently arrived at qualitatively similar results. In the diffusion picture, the mechanistic origin of the pinning-oversaturation stabilization theory is that, when the gas pressure at the bubble-liquid interface is coupled to a gas concentration by Henry's law, the gas flux from the bubble $J \propto -D(c_{\mathrm{bubble}} - c_\infty)$ (where c is the concentration) cancels out when the oversaturation ζ satisfies

$$\zeta = \frac{2\gamma}{LP_0}\sin\theta, \tag{1}$$

where L is the surface nanobubble's footprint radius, θ is the gas-side contact angle, P_0 is the atmospheric pressure, γ is the surface tension, and $\zeta = c_\infty/c_{\mathrm{sat}} - 1$, i.e., the oversaturation is the concentration percentage of gas *throughout the liquid* that is above saturation c_{sat}.

What makes the pinning-oversaturation theory appealing is its prediction that surface nanobubbles can achieve a stable equilibrium, which would naturally address their long lifetimes and unusually small contact angles. A spherical bubble can remain immobile only in an unstable equilibrium—if c_∞ is slightly perturbed from a specific value, it either dissolves completely or grows without bound [1]. On the contrary, the equilibrium achieved in the pinning-oversaturation model for surface nanobubbles is stable, because the bubble will always reach a stationary state when the liquid is sufficiently oversaturated [18].

Despite the aforementioned advances, even state-of-the-art models cannot account for some basic observations which have been known since surface nanobubbles were first discovered. For instance, the pinning-oversaturation model cannot explain why surface nanobubbles are stable in an open environment under standard conditions. This

is because, in an open system, any gas supersaturation produced during nucleation must eventually equilibrate to exact saturation ($\zeta = 0$), which is insufficient to satisfy the Lohse-Zhang stability threshold [as Eq. (1) is positive definite]. However, experiments show that nanobubbles in open systems persist with no imminent sign of dissolution after several days [19]. Existing models also cannot explain the remarkable robustness of the nanobubbles to active degassing ($\zeta < 0$). Rather than dissolving immediately under degassing as theoretically expected, nanobubbles shrink gradually over a timescale of hours [13]. These observations suggest that the pinning-oversaturation description remains incomplete.

In this Letter, we propose that the missing piece in the pinning-oversaturation mechanism is the effect of a hydrophobic attraction on the spatial distribution of the gas adjacent to the solid substrate.

We start by reviewing the derivation of the evolution equation for a dissolving pinned surface nanobubble in a liquid; see Fig. 1(a). This problem is analogous to that of an evaporating droplet of liquid, for which Popov [20] has derived exact analytical equations which are known to agree well with experiments [21]. Adapting Popov's solution, Lohse and Zhang [17] showed that the rate of mass change from a spherical cap nanobubble obeys

$$\frac{dm}{dt} = -\pi L D c_{\mathrm{sat}} f(\theta)\left(\frac{2\gamma}{LP_0}\sin\theta - \zeta\right), \tag{2}$$

where P_0 is the atmospheric pressure, γ is the surface tension, and

$$f(\theta) = \frac{\sin\theta}{1+\cos\theta} + 4\int_0^\infty \frac{1+\cosh 2\theta\xi}{\sinh 2\pi\xi}\tanh[(\pi-\theta)\xi]d\xi \tag{3}$$

is a geometric term which originates from Popov's exact solution [20].

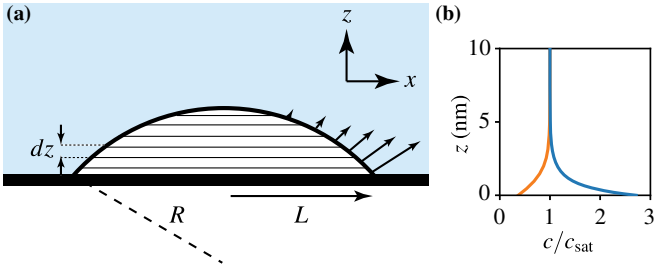

FIG. 1. (a) Schematic of a surface nanobubble. To generalize the gas transport problem to a nonhomogeneous distribution of the dissolved gas concentration, it is helpful to divide the bubble into vertical slices of thickness dz. Ignoring the dissolved gas concentration of the ambient liquid, the bottommost slices have the largest radii and, thus, make the largest contribution to gas exchange. (b) Concentration distribution of the gas as a function of separation z from solid hydrophobic (blue line) and hydrophilic (orange) substrates, based on Eq. (7).

What if the oversaturation ζ is not assumed to be homogeneous throughout the liquid? To generalize the above formulation for *spatially* varying oversaturation $\zeta(z)$, we break up the spherical cap into a series of vertical slices, each with an infinitesimally small height dz [Fig. 1(a)]. The surface area of a spherical cap can be written as the integral $S = 2\pi R\int_0^h dz = 2\pi Rh$, where h is the height of the cap and R the radius of curvature. The driving force for the dissolution is the bubble's Laplace pressure, which is uniformly distributed over its surface. This observation suggests an approach in which we calculate dm/dt by integrating it [and the embedded $\zeta(z)$] over the concentric rings along the z axis and normalizing the result by $S = 2\pi Rh$, leading to the relation

$$\frac{dm}{dt} = -\frac{\pi L D c_{\mathrm{sat}}}{h} f(\theta)\int_0^h \left(\frac{2\gamma}{LP_0}\sin\theta - \zeta(z)\right)dz. \tag{4}$$

Since a spherical cap can be parametrized by its footprint radius L and contact angle θ, the dynamical equation for a pinned surface nanobubble $d\theta/dt$ can be obtained by substituting m out with $m = \pi L^3\rho_g(\cos^3\theta - 3\cos\theta + 2)/3\sin^3\theta$, where ρ_g is the gas density. Surface nanobubbles experience contact line pinning, implemented here by taking the derivative with respect to θ and leaving L constant, giving

$$\frac{d\theta}{dt} = -\frac{D c_{\mathrm{sat}}}{2\rho_g L^2 h}(1+\cos\theta)^2 f(\theta)\int_0^h \left(\frac{2\gamma}{LP_0}\sin\theta - \zeta(z)\right)dz. \tag{5}$$

The height h can be expressed in terms of L and θ from the identity $h = L\sqrt{(1-\cos\theta)/(1+\cos\theta)}$. When $\zeta(z)$ is a constant, Eq. (5) simplifies to the Lohse-Zhang solution [Eq. (10) of Ref. [17]].

In a real system, ζ cannot be taken to be homogeneous throughout the liquid, particularly in the first nanometers away from the solid substrate. Surface force apparatus measurements [22–24] reveal the existence of a short-ranged, exponentially decaying force $F/R_s = -Ce^{-z/\lambda}$ between curved surfaces of radius R_s, where $\lambda \sim 1$ nm is the characteristic distance of the interaction. In other words, the substrate possesses a short-ranged potential $\phi = \phi_0 e^{-z/\lambda}$, which is attractive ($\phi_0 < 0$) for hydrophobic and repulsive ($\phi_0 > 0$) for hydrophilic substrates [24]. While we are not aware of any direct measurement of the interaction strength $|\phi_0|$ of widely used planar substrates, $|\phi_0| \sim k_B T$ is theoretically expected [25,26], and the hydrophobic potential between the amino acid side chains of proteins has also been experimentally measured [27] to be in that range.

If the substrate potential is known, the spatial variation of the gas concentration adjacent to the solid substrate can then be deduced. The diffusive transport of the gas from

a liquid layer of thickness ℓ is governed by the one-dimensional diffusion equation $\partial c/\partial t = D\nabla^2 c$ [28]. The potential interrupts the regular Brownian motion of the gas molecules, modifying the diffusion equation to

$$\frac{\partial c}{\partial t} = D\frac{\partial^2 c}{\partial z^2} + \frac{D}{k_B T}\frac{\partial}{\partial z}\left(c\frac{\partial \phi}{\partial z}\right), \tag{6}$$

known as the Smoluchowski equation [29]. Since nanobubbles appear to be stable over prolonged periods with little change to their shape or size, solving Eq. (6) in the quasisteady limit gives

$$c(z) = c_\infty \exp\left(-\frac{\phi_0 e^{-z/\lambda}}{k_B T}\right). \tag{7}$$

Thus, Eq. (7) predicts a localized buildup in the gas supersaturation next to a hydrophobic solid substrate [blue line, Fig. 1(b)] but a localized undersaturation adjacent to a hydrophilic one (orange line). There is support for a substantial buildup of gas adjacent to a hydrophobic substrate from molecular dynamics (MD) simulations (up to $c/c_{\mathrm{sat}} \approx 100$) [30], though we also note that the gas-infused liquids simulated with MD are often highly supersaturated to begin with [31]. By solving the spatially varying concentration distribution [here, Eq. (7) is recast as an oversaturation $\zeta(z) = c(z)/c_{\mathrm{sat}} - 1$] in conjunction with the dynamical equation for a pinned nanobubble [Eq. (5)], we are able to solve for the dynamical evolution equation of a nanobubble. Throughout this Letter, we use the same parameters as Lohse and Zhang, viz. $D = 2 \times 10^{-9}$ m^2/s, $c_{\mathrm{sat}} = 0.017$ kg/m^3, and $\rho_g = 1.165$ kg/m^3.

In Fig. 2, we show the dynamical evolution of a nanobubble with footprint radius $L = 100$ nm and initial contact angle $\theta = 20°$, in a liquid whose far-field dissolved gas concentration is $c_\infty = 2c_{\mathrm{sat}}$ (or $\zeta = 1$). This degree of gas saturation is typical when nanobubbles are nucleated using the exchange of water and organic solvent. On hydrophobic substrates, the nanobubble achieves an equilibrium contact angle θ_e, but it is unstable on a hydrophilic substrate, due to the evacuation of the gas close to the solid substrate [Fig. 1(b)]. Note that our model preserves the stable equilibrium achieved by the Lohse-Zhang theory. As the nanobubble shrinks on a hydrophobic substrate, its height approaches the thickness of the reservoir of supersaturation, λ, and thus the average supersaturation surrounding the nanobubble increases. We also emphasize here that the geometric factor [Eq. (3)] affects only the duration over which the bubble approaches θ_e but does not influence θ_e itself.

How does the presence of a hydrophobic potential affect the equilibrium contact angle θ_e of a nanobubble with footprint radius L? In Fig. 3, we show plots of $\theta_e(L)$ in the (a) present theory and (b) Lohse-Zhang theory, for the hydrophobic potential $\phi_0/k_B T = -2$. For small L, the contact angles are larger in the current theory than Lohse-Zhang, since θ_e increases with the localized supersaturation surrounding the nanobubbles. The presence of a hydrophobic potential at the solid substrate creates a thin reservoir of gas there which increases θ_e. For large L, θ_e converges to the Lohse-Zhang solution, since the thickness of the reservoir λ becomes negligible compared to the bubble height h.

Our model makes testable predictions about the relationship between θ_e and L. When the supersaturation generated during nucleation is large ($c_\infty/c_{\mathrm{sat}} > 1$), θ_e grows linearly with L, but when it is modest ($c_\infty/c_{\mathrm{sat}} < 1$), the distribution is approximately size independent. There is support for these qualitative features from experiments. The vast majority of experimental investigations study the nucleation of nanobubbles on atomically flat and conductive

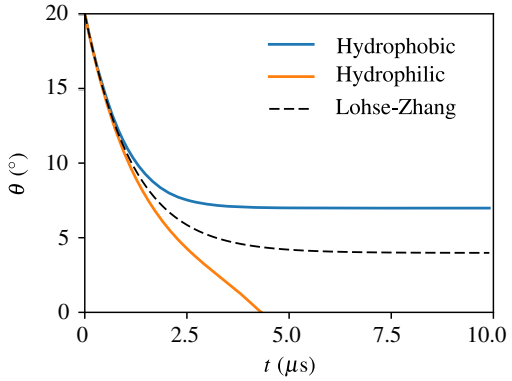

FIG. 2. Dynamical response of a nanobubble with initial footprint radius $L = 100$ nm and initial contact angle $\theta = 20°$ for a liquid with far-field concentration $c_\infty = 2c_{\mathrm{sat}}$. The curves are for hydrophobic ($\phi_0/k_B T = -2$, blue line) and hydrophilic ($\phi_0/k_B T = 2$, orange) substrates in the current theory, and the equivalent condition ($\zeta = 1$) in the Lohse-Zhang theory is shown as a black dashed line.

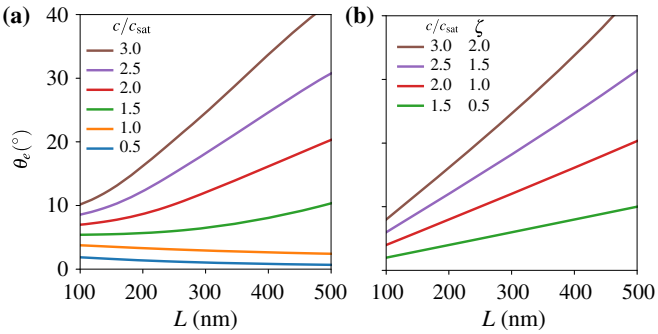

FIG. 3. Equilibrium contact angles of nanobubbles in liquids with varying $c_\infty/c_{\mathrm{sat}}$ in the (a) present theory and (b) Lohse-Zhang theory. Each curve represents one value of dissolved gas concentration $c_\infty/c_{\mathrm{sat}}$ in the liquid. The substrate is assumed hydrophobic ($\phi_0/k_B T = -2$). In the Lohse-Zhang model, nanobubbles are stable only in supersaturated liquid ($c/c_{\mathrm{sat}} > 1$ or $\zeta > 0$).

graphite using atomic force microscopy. When the nucleation is generated by a solvent exchange, which generates a substantial supersaturation $c_\infty/c_{\mathrm{sat}} \approx 2$–$3$, a linearly increasing angle-radius distribution is reported [32,33]. On the other hand, performing electrolysis on the conductive graphite—which should not create a significant supersaturation—generates nanobubbles with nearly size-independent contact angles [34].

Perhaps the most important prediction of our model is that nanobubbles can survive in a degassed liquid. This contrasts with the strict requirement of the Lohse-Zhang theory that the nanobubbles must be in a supersaturated liquid to survive, which is readily contradicted by experiments. Typical protocols to degas liquids require about an hour to reduce the gas concentration in the liquid from saturation, $c_\infty/c_{\mathrm{sat}} \approx 1$ to 0.1–0.2 (see [35]). Since the bulk concentration is below saturation for much of the degassing process, the Lohse-Zhang theory predicts that nanobubbles should promptly disappear after the start of the degassing. However, experiments consistently report that nanobubbles are very robust to degassing, comfortably surviving in an undersaturated liquid with no sign of imminent dissolution even after 20 hr [13]. In our model, the reason for the remarkable robustness of the nanobubbles is that a gas reservoir of supersaturation can still develop adjacent to a hydrophobic substrate, even if the bulk liquid is undersaturated.

We next show how hydrophobicity and supersaturation work together to stabilize surface nanobubbles. In Fig. 4, the equilibrium contact angles θ_e are plotted for $L = 100$ nm as the potential is changed from $-4 \leq \phi_0/k_BT \leq 4$, with the negative (positive) potentials denoting

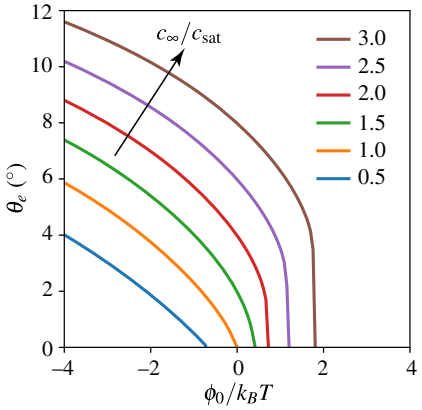

FIG. 4. Equilibrium contact angles of surface nanobubbles with radius $L = 100$ nm as a function of the substrate potential (hydrophobic potentials, $\phi_0 < 0$; hydrophilic potentials, $\phi_0 > 0$). Each curve represents a single value of dissolved gas concentration $c_\infty/c_{\mathrm{sat}}$. Nanobubbles are stable on hydrophobic substrates, and moreover, the equilibrium angle increases with hydrophobicity. In the opposite direction, increasing the hydrophilicity introduces a threshold c_∞ for which stable nanobubbles can be expected.

hydrophobic (hydrophilic) substrates. As expected, nanobubbles are stable when the liquid is supersaturated ($c_\infty/c_{\mathrm{sat}} \geq 1$) and the substrate is hydrophobic. It is also expected that a more hydrophobic substrate simply enhances the buildup of saturation near the substrate and increases the equilibrium contact angle for nanobubbles. However, our model crucially provides the new insight that nanobubbles survive if either supersaturation or hydrophobicity is *absent*, provided that the other variable is large enough to compensate. Figure 4 shows that nanobubbles can remain stable on a moderately hydrophilic surface provided a sufficiently large supersaturation $c_\infty/c_{\mathrm{sat}}$ is present in the bulk liquid. Indeed, fluorescence microscopy experiments by the Ohl group [11,14,18] report stable nanobubbles on hydrophilic glass cover slips.

The idea that the substrate hydrophobicity influences the nanobubble stability dates back to the Brenner-Lohse dynamic equilibrium theory. Given that some of its predictions have been disproved, it is important for us to justify how the current model differs in construction. In the Brenner-Lohse model, the nanobubble's stability is described as a dynamic equilibrium, because the outflux from the nanobubble is at all times compensated by an equivalent influx near the contact line. This construction makes two implicit assumptions: (a) that a net outflux from the bubble is unconditionally present and (b) that the outflux is evenly distributed throughout the bubble surface. Although Brenner and Lohse also derive Eq. (7), the hydrophobic potential is invoked only to argue that an influx of gas would occur at the contact line. Ultimately, an external driving force would be required to sustain both sets of flows simultaneously, but no such mechanism, or reproducible evidence of recirculating flows, has ever been found in experiments [11,12].

How does our model avoid the need for unphysical assumptions? An important insight from the Epstein-Plesset theory and experiments is that bubbles respond dynamically to local changes in the dissolved gas concentration in the surrounding liquid [3,36]. Whether an influx or outflux occurs at the bubble's liquid-gas interface depends on the localized concentration on the liquid side. In our model, the asymmetry in the concentration distribution induced by the hydrophobicity of the solid substrate accounts for both the in- and outfluxes. Regions of the nanobubble within the interaction length scale $z \leq \lambda$ of a hydrophobic substrate experience a net influx, which counteracts the outflux when $z > \lambda$, and the nanobubble achieves equilibrium when the sum of fluxes over the entire bubble is zero. In contrast, the Brenner-Lohse model assumes the unconditional presence of a pressure-driven *outflux at all times*, which must then be compensated by presuming the presence of an influx.

The insights of our work require fresh experimental investigation to compare against. Relatively few papers in the literature focus on the $\theta_e(L)$ size distributions of

the nanobubbles [32,33]. It would be key to repeat these experiments by systematically tuning the hydrophobicity of the substrate. Potentially, this can be achieved by the application of electric fields (utilizing the electrowetting effect) or the chemical treatment of the substrate (such as with silanization). Ultimately, understanding quantitatively how the dissolved gas assembles adjacent to a hydrophobic substrate would require a novel technique to measure the hydrophobic potential of planar substrates.

In summary, we present in this Letter a new theoretical model to understand the stability of surface nanobubbles, by generalizing their diffusive dynamics to incorporate the effects of an attractive hydrophobic potential at the solid substrate. The current theoretical understanding posits that both pinning and supersaturation must be present for nanobubbles to be stabilized but cannot explain why they exist under ambient conditions and why they are so robust to degassing. Our model provides a more nuanced view: While pinning and supersaturation will definitely stabilize nanobubbles, only pinning is mandatory. The degree of saturation and hydrophobicity both contribute to stability, but neither is strictly required—the absence of one can be compensated by an excess of the other.

The surprising influence of the hydrophobic potential brings our understanding of surface nanobubbles full circle to the seminal work of Parker, Claesson, and Attard [37]. Unexpectedly, Parker and colleagues discovered that the force curves between hydrophobic spheres contained discrete steps, though they were expecting a continuous dependence. Their speculation that tiny nanobubbles were mediating a long-ranged attraction is today acknowledged as the starting point for two decades of research in this field. As we now understand it, surface nanobubbles owe their existence to the hydrophobic attraction rather than the other way around.

B. H. T. acknowledges financial support from the Agency of Science, Technology and Research in Singapore. H. A. acknowledges support from the National Key R&D Program of China (2016YFD0400800). We thank Xuehua Zhang and Chenglong Xu for sharing experimental data with us, and we benefited from insightful discussions with Chon U Chan, Qingyun Zeng, and Haibin Su.

*beng@ntu.edu.sg
†hjan@ntu.edu.sg
‡claus-dieter.ohl@ovgu.de

[1] P. S. Epstein and M. S. Plesset, J. Chem. Phys. **18**, 1505 (1950).
[2] L. I. Berge, J. Colloid Interface Sci. **134**, 548 (1990).
[3] P. B. Duncan and D. Needham, Langmuir **20**, 2567 (2004).
[4] D. Lohse and X. Zhang, Rev. Mod. Phys. **87**, 981 (2015).
[5] M. Alheshibri, J. Qian, M. Jehannin, and V. S. J. Craig, Langmuir **32**, 11086 (2016).
[6] V. S. J. Craig, Soft Matter **7**, 40 (2011).
[7] W. A. Ducker, Langmuir **25**, 8907 (2009).
[8] M. P. Brenner and D. Lohse, Phys. Rev. Lett. **101**, 214505 (2008).
[9] J. R. T. Seddon, H. J. W. Zandvliet, and D. Lohse, Phys. Rev. Lett. **107**, 116101 (2011).
[10] S. R. German, X. Wu, H. An, V. S. J. Craig, T. L. Mega, and X. Zhang, ACS Nano **8**, 6193 (2014).
[11] C. U. Chan and C.-D. Ohl, Phys. Rev. Lett. **109**, 174501 (2012).
[12] E. Dietrich, H. J. W. Zandvliet, D. Lohse, and J. R. T. Seddon, J. Phys. Condens. Matter **25**, 184009 (2013).
[13] X. Zhang, D. Y. C. Chan, D. Wang, and N. Maeda, Langmuir **29**, 1017 (2013).
[14] B. H. Tan, H. An, and C.-D. Ohl, Phys. Rev. Lett. **118**, 054501 (2017).
[15] Y. Liu and X. Zhang, J. Chem. Phys. **138**, 014706 (2013).
[16] Y. Liu and X. Zhang, J. Chem. Phys. **141**, 134702 (2014).
[17] D. Lohse and X. Zhang, Phys. Rev. E **91**, 031003 (2015).
[18] C. U. Chan, M. Arora, and C.-D. Ohl, Langmuir **31**, 7041 (2015).
[19] H. An, B. H. Tan, Q. Zeng, and C.-D. Ohl, Langmuir **32**, 11212 (2016).
[20] Y. O. Popov, Phys. Rev. E **71**, 036313 (2005).
[21] H. Gelderblom, A. G. Marín, H. Nair, A. van Houselt, L. Lefferts, J. H. Snoeijer, and D. Lohse, Phys. Rev. E **83**, 026306 (2011).
[22] J. N. Israelachvili and R. M. Pashley, J. Colloid Interface Sci. **98**, 500 (1984).
[23] M. U. Hammer, T. H. Anderson, A. Chaimovich, M. S. Shell, and J. Israelachvili, Faraday Discuss. **146**, 299 (2010).
[24] S. H. Donaldson, A. Røyne, K. Kristiansen, M. V. Rapp, S. Das, M. A. Gebbie, D. W. Lee, P. Stock, M. Valtiner, and J. Israelachvili, Langmuir **31**, 2051 (2015).
[25] B. Widom, P. Bhimalapuram, and K. Koga, Phys. Chem. Chem. Phys. **5**, 3085 (2003).
[26] S. Shimizu and H. S. Chan, J. Chem. Phys. **113**, 4683 (2000).
[27] H. A. Scheraga, J. Biomol. Struct. Dyn. **16**, 447 (1998).
[28] J. H. Weijs and D. Lohse, Phys. Rev. Lett. **110**, 054501 (2013).
[29] M. Doi and S. F. Edwards, *The Theory of Polymer Dynamics* (Oxford University, New York, 1988), Vol. 73, Chap. 3.
[30] S. M. Dammer and D. Lohse, Phys. Rev. Lett. **96**, 206101 (2006).
[31] Most gases have a solubility in water of ∼10 particles per million. As a statistically significant simulation of a bubble containing just ∼100–1000 gas molecules is too computationally demanding, most computational studies of this kind compromise by simulating highly supersaturated liquids.
[32] C. Xu, S. Peng, G. G. Qiao, V. Gutowski, D. Lohse, and X. Zhang, Soft Matter **10**, 7857 (2014).
[33] L. Zhang, X. Zhang, Y. Zhang, J. Hu, and H. Fang, Soft Matter **6**, 4515 (2010).
[34] H. An, B. H. Tan, and C.-D. Ohl, Langmuir **32**, 12710 (2016).
[35] I. B. Butler, M. A. A. Schoonen, and D. T. Rickard, Talanta **41**, 211 (1994).
[36] T. Yamashita and K. Ando, J. Fluid Mech. **825**, 16 (2017).
[37] J. L. Parker, P. M. Claesson, and P. Attard, J. Phys. Chem. **98**, 8468 (1994).